

## Chaos and Quantum Irreversibility

Roberto Roncaglia,<sup>1</sup> Luca Bonci,<sup>1,2</sup> Paolo Grigolini,<sup>1,2</sup> and Bruce J. West<sup>1</sup>

*Received October 2, 1991; final January 28, 1992*

---

We study the Hamiltonian of a two-level system interacting with a one-mode radiation field by means of the Wigner method and without using the rotating-wave approximation. We show that a phenomenon of collapses and revival, reminiscent of that exhibited by the Jaynes-Cummings model, takes place in the high-coupling limit. This process appears as irreversible or virtually reversible, according to whether the semiclassical regime is chaotic or not. Thus, we find a new mechanism for dissipation in the quantum domain.

---

**KEY WORDS:** Chaos; quantum irreversibility; spin-boson Hamiltonian; Wigner distribution.

### 1. INTRODUCTION

Since the 1975 paper of Li and York<sup>(1)</sup> in which the term chaos was introduced, this dynamical concept has steadily found increasing application in understanding all manner of natural phenomena.<sup>(2-5)</sup> Chaotic motion is an implicit property of nonlinear systems arising in discrete mappings<sup>(6)</sup> and in continuous low-dimensional dynamical equations<sup>(7)</sup> representing classical phenomena. Its precise mathematical definition is still somewhat flexible, but does entail a sensitive dependence on initial conditions for a deterministic, nonlinear dynamical system and solutions to these equations that are highly irregular, i.e., random.<sup>(8)</sup> The macroscopic world of the weather,<sup>(9)</sup> the heart,<sup>(10)</sup> and the growth of populations<sup>(11)</sup> all seem to be strongly influenced by chaos. Herein we use a model system to examine how chaos in the macroscopic domain manifests itself in the microscopic, which is to say how the system properties leading to the existence of chaotic solutions in the semiclassical description of the dynamics are manifest in the corresponding fully quantum mechanical description.

---

<sup>1</sup> Department of Physics, University of North Texas, P.O. Box 5368, Denton, Texas 76203.

<sup>2</sup> Dipartimento di Fisica dell'Università di Pisa, Piazza Torricelli, 56100 Pisa, Italy.

In Section 2 we apply the Wigner distribution method to the quantum system of a two-level spin coupled to a coherent field. The semiclassical equations for this spin-boson system can have chaotic solutions in certain parameter regimes. It is found that the *Liouillian* determining the evolution of the Wigner distribution has two parts, one containing this semiclassical behavior and the other arising from purely quantum effects; the two effects compete against one another.<sup>(14,15)</sup> A reduced Wigner distribution is introduced in Section 3 in order to provide a systematic approximation scheme for numerically integrating the quantum and semiclassical equations of motion. In Section 4 it is shown using the Lyapunov exponents that the spin-boson system is ergodic in the parameter regions where the solutions to the semiclassical equations are chaotic.

The numerical integration of both the exact quantum mechanical equations and the semiclassical equations for the spin-boson system is discussed in Section 5. Therein it is demonstrated by means of the entropy for the spin subsystem that the full nonlinear dynamic equations destroy the phenomenon of "collapse and revival" of the wave function,<sup>(16-20)</sup> which suggests that chaos leads to quantum irreversibility, i.e., that quantum dissipation need not be a many-body effect, but can also be a manifestation of chaos in the quantum domain.<sup>(15)</sup> In Section 6 we record the salient conclusions from the present investigation.

## 2. SPIN-BOSON HAMILTONIAN

Let us examine the application of the Wigner distribution method to a quantum mechanical system of sufficient complexity that its semiclassical equations of motion have chaotic solutions. We investigate one of the simplest such systems, the spin-boson Hamiltonian:

$$\hat{H} = -\frac{1}{2} \omega_0 \hat{\sigma}_z + \frac{g}{(2\Omega)^{1/2}} \hat{\sigma}_x (\hat{b} + \hat{b}^\dagger) + \Omega \hat{b}^\dagger \hat{b} \quad (2.1)$$

where  $\hat{b}$  ( $\hat{b}^\dagger$ ) is the annihilation (creation) operator with commutation  $[\hat{b}, \hat{b}^\dagger] = 1$ ;  $\hat{q} = (\hat{b} + \hat{b}^\dagger)/(2\Omega)^{1/2}$  and  $\hat{p} = i(\hat{b}^\dagger - \hat{b})(\Omega/2)^{1/2}$  are the coordinate and momentum operators of our oscillator with frequency  $\Omega$ ; and  $\hat{\sigma}_x$  and  $\hat{\sigma}_z$  are spin matrices. Herein we study the dynamics of the spin-boson system with the initial condition

$$\hat{\sigma}_z |\pm\rangle = \pm |\pm\rangle \quad (2.2)$$

and the boson field is a coherent state characterized by the average number of photons  $\langle n \rangle$ . The equations of motion for this system are analogous to the quantum optics model of Jaynes and Cummings (JCM) for a two-state

atom interacting with the single mode of an electric field<sup>(22)</sup> in the rotating wave approximation (RWA) of (2.1). As written, (2.1) describes a spin-1/2 dipole in a single-mode magnetic field directed along the  $z$  axis. A system of this kind has recently been studied by Graham and Höhnerbach.<sup>(23)</sup> They show that a semiclassical approximation of this system exhibits chaotic dynamics for sufficiently strong coupling  $g$ . Similar results have been found by Belorov *et al.*<sup>(24)</sup> and Milonni *et al.*<sup>(25)</sup> A brief discussion of the present analysis has been given by Bonci *et al.*<sup>(15)</sup>

The question we address here is: What is the influence of the classically chaotic trajectories on the solutions to the Schrödinger equation?

We shed some light on this difficult question using the phase space methods of ref. 13. We extend the arguments used earlier<sup>(13)</sup> so as to be applicable to the spin-boson problem. For this system the pseudo-probability function reads

$$\rho_w(\mathbf{x}, q, p; t) = \int \frac{e^{-i\mathbf{k} \cdot \mathbf{x}}}{(2\pi)^3} d\mathbf{k} \int \frac{e^{-(iq\alpha + p\tau)}}{(2\pi)^2} dq dp F(\mathbf{k}, \alpha, \tau; t) \quad (2.3)$$

where  $F(\mathbf{k}, \alpha, \tau; t)$  is the quantum characteristic function defined by

$$F(\mathbf{k}, \alpha, \tau; t) = \text{Tr} \{ e^{i(k_1 \hat{\sigma}_x + k_2 \hat{\sigma}_y + k_3 \hat{\sigma}_z)} e^{i(\alpha \hat{q} + \tau \hat{p})} \hat{\rho}(t) \} \quad (2.4)$$

where  $\hat{\rho}(t)$  is the density operator for the complete system. Note that (2.3) and (2.4) extend the usual treatment of the Wigner distribution to include spin.

The variables  $\mathbf{x} = (x_1, x_2, x_3)$ ,  $p$ , and  $q$  are the phase-space variables associated, via a generalized Weyl rule,<sup>(21)</sup> to the spin-boson operators:  $\hat{\sigma}_j \rightarrow x_j$ ,  $\hat{q} \rightarrow q$ , and  $\hat{p} \rightarrow p$ .<sup>(14,15)</sup> The average values of these operators on the statistical system described by the density matrix  $\hat{\rho}$  are given by

$$\langle \hat{\sigma}_j \rangle(t) = \int d\mathbf{x} dq dp x_j \rho_w(\mathbf{x}, q, p; t) \quad (2.5a)$$

$$\langle \hat{q} \rangle(t) = \int d\mathbf{x} dq dp q \rho_w(\mathbf{x}, q, p; t) \quad (2.5b)$$

The equation of evolution for the Wigner distribution (2.3) is given by

$$\frac{\partial}{\partial t} \rho_w(\mathbf{x}, q, p; t) = (\hat{\mathcal{L}}_{cl} + \hat{\mathcal{L}}_{QGD}) \rho_w(\mathbf{x}, q, p; t) \quad (2.6)$$

where, after some substantial algebra,

$$\begin{aligned} \hat{\mathcal{L}}_{cl} \equiv & \omega_0 \left( x_1 \frac{\partial}{\partial x_2} - x_2 \frac{\partial}{\partial x_1} \right) + 2gq \left( x_3 \frac{\partial}{\partial x_2} - x_2 \frac{\partial}{\partial x_3} \right) \\ & + \Omega^2 q \frac{\partial}{\partial p} - p \frac{\partial}{\partial q} + gx_1 \frac{\partial}{\partial p} \end{aligned} \quad (2.7)$$

and

$$\mathcal{L}_{\text{QGD}} \equiv g \frac{\partial}{\partial p} \left[ \frac{\partial}{\partial x_1} - \frac{\partial}{\partial x_1} x_1^2 - \frac{\partial}{\partial x_2} x_1 x_2 - \frac{\partial}{\partial x_3} x_1 x_3 \right] \quad (2.8)$$

The operator  $\mathcal{L}_{\text{cl}}$  is identical to the Liouvillian of a classical dipole interacting with a classical oscillator, i.e., this term alone corresponds to the semiclassical set of equations discussed by various authors.<sup>(26)</sup> We refer to the calculations based on the study of the single trajectory solutions of the nonlinear dynamical equations as the semiclassical predictions. In this regard we point out a significant feature of the analysis that was apparently overlooked in previous investigations having to do with chaotic trajectories.<sup>(22-25)</sup> These earlier studies focused on individual trajectories and gave them physical meaning; however, from (2.5) even when  $\mathcal{L}_{\text{QGD}}$  is neglected, it is only the ensemble that has physical significance, not the individual trajectories.<sup>(15)</sup>

The term  $\mathcal{L}_{\text{QGD}}$  in (2.8) has a number of significant implications. First of all, since spin does not have a classical analogue, the classical limit is not obtained by taking the  $\hbar \rightarrow 0$  limit as one would in a strictly  $(q, p)$  system. Furthermore, the  $\mathcal{L}_{\text{QGD}}$  operator does not explicitly contain  $\hbar$ . Second,  $\mathcal{L}_{\text{QGD}}$  has a diffusion-like structure, but the state dependence of the "diffusion coefficient" results in its not being positive-definite. It has recently been shown by Roncaglia *et al.*<sup>(14)</sup> that if the oscillator is coupled to a heat bath so as to transmit to the spin-1/2 dipole standard thermal fluctuations, then this term results in the average value of the  $z$  component of the dipole changing from a Langevin (classical) function to the hyperbolic tangent (quantum). In other words, this term, coined the quantization generating diffusion (QGD) by these authors,<sup>(14)</sup> ensures that the dipole retains its quantum nature. The operator  $\mathcal{L}_{\text{QGD}}$  acts as an antidiffusional mechanism; it competes against thermal fluctuations and constrains the dipole, which otherwise would freely diffuse over all possible orientations, to vacillate between two possible orientations. It seems that in the absence of diffusion this term is inactive; it is only activated with the onset fluctuations, either thermally or chaotically induced.

The explicit form of the nonlinear equations of motion given by the Hamiltonian (2.1) is

$$\begin{aligned} \dot{x}_1 &= \omega_0 x_2 \\ \dot{x}_2 &= -\omega_0 x_1 - 2ge^{f_1} x_3 q \\ \dot{x}_3 &= 2ge^{f_1} x_2 q \\ \dot{q} &= p \\ \dot{p} &= -\Omega^2 q - gx_1 \end{aligned} \quad (2.9)$$

Note that these equations describe the evolution of the spin-boson system using the phase space variables and not the quantum mechanical operators. We now wish to solve these equations, at least within some systematic approximation scheme. A rigorous analysis of (2.9) could treat the terms

$$e^{\hat{r}^t x_3 q} \quad \text{and} \quad e^{\hat{r}^t x_2 q}$$

as additional variables and in this way the dynamical equations for these variables would be extended to the same infinite set of linear differential equations that one would obtain using the Heisenberg picture. The most direct way to truncate the infinite hierarchy of linear differential equations is to make the following approximation:

$$e^{\hat{r}^t x_j q} \cong (e^{\hat{r}^t x_j})(e^{\hat{r}^t q}) \tag{2.10}$$

It is important to appreciate that although (2.10) resembles the semi-classical factorization

$$\langle \hat{\sigma}_j \hat{q} \rangle(t) \cong \langle \hat{\sigma}_j \rangle(t) \langle \hat{q} \rangle(t) \tag{2.11}$$

it is in fact quite different. Equation (2.11) applies to the breaking of correlations in the averages over the quantum mechanical variables, whereas (2.10) applies the analogous factorization assumption to a single trajectory. Once we neglect the contribution of  $\mathcal{L}_{\text{QGD}}$  in (2.10), the evolution of the quantum system evolves by means of  $\mathcal{L}_{\text{cl}}$ , the classical deterministic operator, only. Thus, in this approximation scheme the only difference between the classical and quantum systems is due to the fact that the quantum averages are obtained using the phase space averages, i.e., averaging the classical trajectories over the appropriate pseudo-probability density. We apply this approximation method to the spin-boson system. More specifically, we solve the classical system of equations (2.9) by numerical integration and average the classical trajectories over the proper distribution function.

To carry out the above program, we address the subtle problem of the form of the Wigner distribution for the spin-boson Hamiltonian. We analyze this in detail in the next section.

### 3. SPIN-BOSON REDUCED WIGNER DISTRIBUTION

The quantum mechanical density matrix for the spin-boson system is written as follows:

$$\hat{\rho}(t) = \frac{1}{2} \hat{\sigma}_0 \hat{\rho}_0(\hat{q}, \hat{p}; t) + \sum_{j=1}^3 \frac{1}{2} \hat{\sigma}_j \hat{\rho}_j(\hat{q}, \hat{p}; t) \tag{3.1}$$

where  $\hat{\sigma}_0$  is the  $2 \times 2$  identity matrix,  $\hat{\sigma}_j$  ( $j=1, 2, 3$ ) are the Pauli spin matrices, and  $\hat{\rho}_j(t)$  ( $j=1, 2, 3$ ) are the reduced density matrices defined as

$$\hat{\rho}_0(t) \equiv \text{Tr}_{\text{spin}} [\hat{\rho}(\hat{\mathbf{c}}, \hat{q}, \hat{p}; t)] \quad (3.2)$$

$$\hat{\rho}_j(t) \equiv \text{Tr}_{\text{spin}} [\hat{\sigma}_j \hat{\rho}(\hat{\mathbf{c}}, \hat{q}, \hat{p}; t)] \quad (3.3)$$

If we substitute the density matrix (3.1) into (2.4) and then into (2.3) and use polar coordinates for the spin variables  $x_j$ , we obtain the most general Wigner distribution:

$$\begin{aligned} \rho_w(\mathbf{x}, q, p; t) = & \frac{1}{4\pi} \frac{1}{x} \frac{\partial}{\partial x} \delta(1-x) \rho_{w,0}(q, p; t) \\ & - \frac{1}{4\pi} \sin \theta \cos \phi \frac{\partial}{\partial x} \delta(1-x) \rho_{w,1}(q, p; t) \\ & - \frac{1}{4\pi} \sin \theta \sin \phi \frac{\partial}{\partial x} \delta(1-x) \rho_{w,2}(q, p; t) \\ & - \frac{1}{4\pi} \cos \theta \frac{\partial}{\partial x} \delta(1-x) \rho_{w,3}(q, p; t) \end{aligned} \quad (3.4)$$

where

$$x = (x_1^2 + x_2^2 + x_3^2)^{1/2} \quad (3.5)$$

and the  $\rho_{wj}$  are the contributions to the Wigner distribution associated with the reduced density matrices (3.2) and (3.3). Thus, it is straightforward to show that the time-dependent averages of interest are given by

$$\begin{aligned} \text{Tr}[\hat{\sigma}_j \hat{\rho}(t)] &= \int dq \int dp \rho_{wj}(q, p; t), \quad j=1, 2, 3 \\ \text{Tr}[\hat{\rho}(t)] &= \int dq \int dp \rho_{w,0}(q, p; t) \\ \text{Tr}[\hat{q} \hat{\rho}(t)] &= \int dq \int dp q \rho_{w,0}(q, p; t) \\ \text{Tr}[\hat{p} \hat{\rho}(t)] &= \int dq \int dp p \rho_{w,0}(q, p; t) \end{aligned} \quad (3.6)$$

It is clear from (3.4) and the averages in (3.6) that the total Wigner distribution is primarily of mathematical interest only, while the physical

quantities of interest are obtained using the reduced Wigner distributions  $\rho_{wj}$ . Said differently, we cannot use (3.4) to numerically calculate the quantities of interest, whereas the reduced distributions in (3.6) directly lend themselves to computer calculations. To see this, we avoid using  $\rho_w$  and determine the equations of evolution for the  $\rho_{wj}$ . First, we eliminate the nonphysical part of the Wigner distribution by integrating  $\rho_w(\mathbf{x}, q, p; t)$  over all possible lengths  $x$  of the quantum dipole:

$$\tilde{\rho}_w(\theta, \phi, q, p; t) = \int_0^1 dx x^2 \rho_w(x, \theta, \phi, q, p; t) \quad (3.7)$$

Second, we define the contracted Liouvillian  $\tilde{\mathcal{L}}$  as follows:

$$\frac{\partial}{\partial t} \tilde{\rho}_w = \tilde{\mathcal{L}} \tilde{\rho}_w \equiv \int_0^\infty dx x^2 \tilde{\mathcal{L}} \rho_w(x, \theta, \phi, q, p; t) \quad (3.8)$$

After straightforward but rather tedious calculations, we find

$$\begin{aligned} \tilde{\mathcal{L}} \tilde{\rho}_w = & \frac{1}{4\pi} \left( -p \frac{\partial}{\partial q} + \Omega^2 q \frac{\partial}{\partial p} \right) \rho_{w,0} + \frac{q}{4\pi} \frac{\partial}{\partial p} \rho_{w1} \\ & + \frac{\sin \theta \cos \theta}{2\pi} \left\{ \left( -p \frac{\partial}{\partial q} + \Omega^2 q \frac{\partial}{\partial p} \right) \rho_{w1} + g \frac{\partial}{\partial p} \rho_{w0} + \omega_0 \rho_{w2} \right\} \\ & + \frac{\sin \theta \sin \phi}{2\pi} \left\{ \left( -p \frac{\partial}{\partial q} + \Omega^2 q \frac{\partial}{\partial p} \right) \rho_{w2} - \omega_0 \rho_{w1} - 2gq \rho_{w3} \right\} \\ & + \frac{\cos \theta}{2\pi} \left\{ \left( -p \frac{\partial}{\partial q} + \Omega^2 q \frac{\partial}{\partial p} \right) \rho_{w3} + 2gq \rho_{w2} \right\} \end{aligned} \quad (3.9)$$

Finally, comparing (3.9) with (3.8) gives the result

$$\frac{\partial}{\partial t} \rho_{w0} = \left( -p \frac{\partial}{\partial q} + \Omega^2 q \frac{\partial}{\partial p} \right) \rho_{w0} + g \frac{\partial}{\partial p} \rho_{w1} \quad (3.10a)$$

$$\frac{\partial}{\partial t} \rho_{w1} = \left( -p \frac{\partial}{\partial q} + \Omega^2 q \frac{\partial}{\partial p} \right) \rho_{w1} + g \frac{\partial}{\partial p} \rho_{w0} + \omega_0 \rho_{w2} \quad (3.10b)$$

$$\frac{\partial}{\partial t} \rho_{w2} = \left( -p \frac{\partial}{\partial q} + \Omega^2 q \frac{\partial}{\partial p} \right) \rho_{w2} - \omega_0 \rho_{w1} - 2gq \rho_{w3} \quad (3.10c)$$

$$\frac{\partial}{\partial t} \rho_{w3} = \left( -p \frac{\partial}{\partial q} + \Omega^2 q \frac{\partial}{\partial p} \right) \rho_{w3} + 2gq \rho_{w2} \quad (3.10d)$$

Note that this set of four partial differential equations is *exact*. The solution to this set of equations is completely equivalent to that of the quantum

spin-boson problem. We also emphasize that the mathematical structure of (3.10) for the reduced Wigner distributions is quite different from that obtained for  $\rho_w$  itself.<sup>(13)</sup>

We now reformulate the dynamical equations for the  $\rho_{wj}$  into a more familiar representation. We define the *probability vector* as

$$|\rho_w(q, p; t)\rangle = \rho_{w0}(q, p; t) |0\rangle + \rho_{w1}(q, p; t) |1\rangle + \rho_{w2}(q, p; t) |2\rangle + \rho_{w3}(q, p; t) |3\rangle \quad (3.11)$$

where the vector  $|j\rangle$  satisfies the orthonormality condition

$$\langle j | k \rangle = \delta_{j,k}, \quad j, k = 0, 1, 2, 3 \quad (3.12)$$

Equations (3.10) recover the Liouville-like form

$$\frac{\partial}{\partial t} |\rho_w(q, p; t)\rangle = \hat{A} |\rho_w(q, p; t)\rangle \quad (3.13)$$

where

$$\hat{A} = \left( -p \frac{\partial}{\partial q} + \Omega^2 q \frac{\partial}{\partial p} \right) \hat{\sigma}_0 + g \frac{\partial}{\partial p} (|0\rangle\langle 1| + |1\rangle\langle 0|) - \omega_0 (|2\rangle\langle 1| - |1\rangle\langle 2|) - 2gq (|2\rangle\langle 3| - |3\rangle\langle 2|) \quad (3.14)$$

In this formalism, to any quantum observable  $\hat{A}$  is associated a vector  $|A\rangle$  and its time-dependent expectation value:

$$\langle \hat{A} \rangle(t) = \int dq \int dp \langle A | \exp(\hat{A}t) | \rho_w(q, p; 0) \rangle \quad (3.15)$$

This allows us to define an evolution operator for the *observable*  $|A\rangle$ :

$$\int dq \int dp \langle A | \exp(\hat{A}t) | \rho_w \rangle = \int dq \int dp \langle A(t) | \rho_w \rangle \quad (3.16)$$

where

$$|\hat{A}(t)\rangle = \exp(\hat{F}t) |A\rangle \quad (3.17)$$

Note that  $\hat{F}$  is the adjoint to  $\hat{A}$ , so that

$$\hat{F} = -\hat{A} \quad (3.18)$$

The next step consists in making the assumption that the initial density matrix of the spin-boson Hamiltonian factors,

$$\hat{\rho}(t=0) = \frac{1}{2} \left( \hat{\sigma}_0 + \sum_{j=1}^3 \langle \hat{\sigma}_j \rangle \hat{\sigma}_j \right) \hat{\rho}_B(\hat{q}, \hat{p}; t=0) \quad (3.19)$$



where  $\hat{\rho}_B(\hat{q}, \hat{p}; t=0)$  denotes the oscillator density matrix at the initial time  $t=0$ . The probability vector (3.11) corresponding to this state is

$$|\rho_w\rangle = \rho_{Bw}(q, p) \left[ |0\rangle + \sum_{j=1}^3 \langle \hat{\sigma}_j(0) \rangle |j\rangle \right] \tag{3.20}$$

where  $\rho_{Bw}(q, p)$  is the Wigner distribution corresponding to the density matrix  $\hat{\rho}_B(\hat{q}, \hat{p})$ . Note that the initial conditions on the spin-1/2 system are expressed in terms of the state vector:

$$|\pi\rangle = \left[ |0\rangle + \sum_{j=1}^3 \langle \hat{\sigma}_j(0) \rangle |j\rangle \right] \tag{3.21}$$

Using (3.16) and (3.20), we obtain

$$\langle \hat{A} \rangle(t) = \int dq \int dp \rho_{Bw}(q, p) \langle \pi | \exp(\hat{F}t) | A \rangle \tag{3.22}$$

where the scalar product  $\langle \pi | \exp(\hat{F}t) | A \rangle$  is a function of the *initial coordinates*  $p$  and  $q$ , as is evident from the definition of  $\hat{F}$ . The quantum result is obtained from (3.22) by averaging the single trajectory  $\langle \pi | \exp(\hat{F}t) | A \rangle$  over the ensemble distribution of initial conditions for the mode of the electric field. It is important to note that the distribution function  $\rho_{Bw}(q, p)$  in (3.22) is always well-behaved. To complete this procedure, we need the equations of motion for the trajectories  $\langle \pi | \exp(\hat{F}t) | A \rangle$ .

As in (2.5), we are interested in the evolution of the spin operators. This leads us to the definitions

$$\begin{aligned} x_j(q, p; t) &= \langle \pi | \exp(\hat{F}t) | j \rangle \\ q(q, p; t) &= \langle \pi | [\exp(\hat{F}t)] q | 0 \rangle \\ p(q, p; t) &= \langle \pi | [\exp(\hat{F}t)] p | 0 \rangle \end{aligned} \tag{3.23}$$

so the equations of motion for these variables are

$$\begin{aligned} \dot{x}_1(t) &= \omega_0 x_2(t) \\ \dot{x}_2(t) &= -\omega_0 x_1(t) - 2g \langle \pi | [\exp(\hat{F}t)] q | 3 \rangle \\ \dot{x}_3(t) &= 2g \langle \pi | [\exp(\hat{F}t)] q | 2 \rangle \\ \dot{q}(t) &= p(t) \\ \dot{p}(t) &= -\Omega^2 q(t) - g x_1(t) \end{aligned} \tag{3.24}$$

where the initial conditions are

$$\begin{aligned}x_j(q, p; 0) &= \langle \hat{\sigma}_j \rangle(0) \\q(q, p; 0) &= q \\p(q, p; 0) &= p\end{aligned}\tag{3.25}$$

We see that like (2.5), the dynamic equations (3.24) are not closed. In the Appendix we demonstrate that

$$\begin{aligned}\langle \pi | [\exp(\hat{F}t)] q | 3 \rangle &\cong \langle \pi | [\exp(\hat{F}t)] q | 0 \rangle \langle \pi | \exp(\hat{F}t) | 3 \rangle \\ \langle \pi | [\exp(\hat{F}t)] q | 2 \rangle &\cong \langle \pi | [\exp(\hat{F}t)] q | 0 \rangle \langle \pi | \exp(\hat{F}t) | 2 \rangle\end{aligned}\tag{3.26}$$

which is equivalent to neglecting the contribution of  $\hat{\mathcal{L}}_{\text{QGD}}$  in (2.6). This factorization leads to a closed set of classical equations that are correct to first order in the coupling constant  $g$ . A more complete discussion of this approximation in the resonant case ( $\omega_0 = \Omega$ ) is given in the Appendix. Equations (3.24) in this approximation are

$$\begin{aligned}\dot{x}_1(t) &= \omega_0 x_2(t) \\ \dot{x}_2(t) &= -\omega_0 x_1(t) - 2gq(t) x_3(t) \\ \dot{x}_3(t) &= 2gq(t) x_2(t) \\ \dot{q}(t) &= p(t) \\ \dot{p}(t) &= -\Omega^2 q(t) - gx_1(t)\end{aligned}\tag{3.27}$$

which can be numerically integrated.

This completes our approximation scheme. We integrate (3.27) to obtain the quantum result by averaging the classical trajectories over the following distribution of initial conditions:

$$\begin{aligned}\rho_w(x, q, p; t=0) \\ = \rho_{Bw}(q, p) \delta(x_1 - \langle \hat{\sigma}_1 \rangle) \delta(x_2 - \langle \hat{\sigma}_2 \rangle) \delta(x_3 - \langle \hat{\sigma}_3 \rangle)\end{aligned}\tag{3.28}$$

In the initial state the spin is specified separately from the coherent field and the two are assumed to have not as yet interacted.

#### 4. ERGODICITY AND CHAOS

In this section we analyze the behavior of the classical system obtained from the spin-boson Hamiltonian. As we pointed out earlier, the solution to the system (3.27) is chaotic for a certain range of parameter values. This

means that trajectories starting close together in phase separate exponentially and this initial correlation is lost after a certain time. An important aspect of this semiclassical chaos is the appearance of relaxation properties which are, in principle, unexpected in a system with a limited number of degrees of freedom. This is just the kind of system we have, two states for the spin-1/2 dipole and an oscillator representing the electric field. Therefore we would be tempted to say that the original semiclassical chaos, manifesting itself through erratic trajectories, is now replaced by a single regular but dissipative trajectory.

One of the most widely accepted indicators of chaotic motion is the Lyapunov exponent for the trajectory.<sup>(27)</sup> In common practice the mean exponential rate of divergence of two initially adjacent trajectories is given by the Lyapunov exponent. For an  $M$ -dimensional set of differential equations the definition of the Lyapunov exponent is

$$\gamma(x_0, \omega) = \lim_{t \rightarrow \infty} \frac{1}{t} \ln \left[ \frac{d(x_0, t)}{d(x_0, 0)} \right], \quad d(0) \rightarrow 0 \quad (4.1)$$

where the separation between two initially adjacent trajectories at time  $t$  is

$$d(x_0, t) = \|X(x_0 + \varepsilon\omega, t) - X(x_0, t)\| \quad (4.2)$$

where  $\|\cdot\|$  denotes the norm. Here  $X(x_0, t)$  is the trajectory at time  $t$  and  $X(x_0, t=0) = x_0$ . Further,  $\varepsilon \ll 1$  and  $\|\omega\| = 1$ . It is possible to show that there are  $M$ , possibly nondistinct, Lyapunov exponents, corresponding to the  $M$  possibly independent directions of  $\omega$ , and these do not depend on the choice of metric for the space.

The computation of the Lyapunov exponent is, in general, a nontrivial task. It is much easier to obtain the largest exponent for a given trajectory. Using the method of Benettin *et al.*,<sup>(28)</sup> we have calculated this exponent for different values of the parameters. The main computational results can be summarized as follows:

1. The trajectories have the greatest Lyapunov exponents in the resonant case,  $\Omega = \omega_0$ . In Fig. 1 we see that the exponents are negligibly small and positive for the coupling coefficient  $g \leq 10$ . There is, however, a threshold in the largest Lyapunov value in the neighborhood of  $g = 11$ , after which the exponent clearly becomes large and positive. The dependence of the largest Lyapunov exponent is an increasing function of  $g$  on the average. We conclude from this figure that the trajectories are regular for  $g \leq 10$  and chaotic for  $g \geq 11$ .

2. When the spin-boson system is no longer in resonance ( $\omega_0 \neq \Omega$ ) the largest exponent is on the order of 0.1 for most values of  $g$ , including those that are very large.

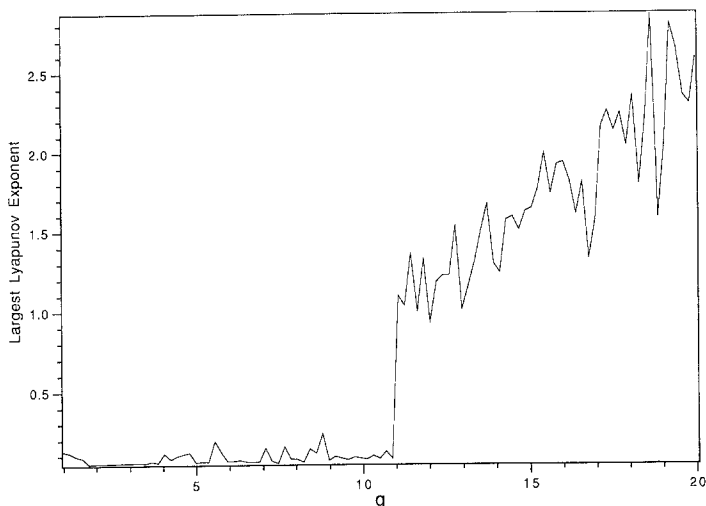


Fig. 1. The largest Lyapunov exponent of the set of differential equations (3.27) as a function of the coupling strength  $g$ . The parameters used are  $\omega_0 = \Omega = 2\pi$  and  $\bar{n} = 5$ .

The *Berry-Vorhos hypothesis* states that the Wigner distribution for the stationary state of an ergodic system is given by the microcanonical distribution.<sup>(29,30)</sup> We directly verify this hypothesis in the present case by noting that a system is called ergodic if the time average and the phase space average are equal. If  $f(y)$  is an integrable function of a representative phase space point  $y$ , then the time average is

$$\langle f \rangle_T = \lim_{T \rightarrow \infty} \frac{1}{T} \int_{t_0}^{t_0+T} f(y(t)) dt \quad (4.3)$$

and the phase space average is

$$\langle f \rangle_S = \frac{1}{\Sigma(E)} \int_{S_E} f(y) dS_E = \frac{1}{\Sigma(E)} \int \delta(H(y) - E) dy \quad (4.4)$$

where  $dS_E$  is an element of area on a surface of constant energy, which is invariant during the evolution of the system. The quantity  $\Sigma(E)$  is the total area of the constant-energy surface and is defined as

$$\Sigma(E) = \int_{S_E} dS_E = \int \delta(H(y) - E) dy \quad (4.5)$$

and is the normalization constant in (4.4).

To understand the relation between time and space averages of the spin-boson system, we calculate the phase space average of the  $z$  component of the spin:

$$\begin{aligned} \langle \hat{\sigma}_z \rangle_s = & \left[ \int dq \int dp \int d\theta \int d\phi \sin \theta \cos \theta \right. \\ & \times \left. \delta(E + \frac{1}{2}\omega_0 \cos \theta - gq \sin \theta \cos \phi - \frac{1}{2}\Omega^2 q^2 - \frac{1}{2}p^2) \right] \\ & \times \left[ \int dq \int dp \int d\theta \int d\phi \sin \theta \right. \\ & \times \left. \delta(E + \frac{1}{2}\omega_0 \cos \theta - gq \sin \theta \cos \phi - \frac{1}{2}\Omega^2 q^2 - \frac{1}{2}p^2) \right]^{-1} \end{aligned} \quad (4.6)$$

The integration over the variables  $q$  and  $p$  can be carried out easily and yields

$$\langle \hat{\sigma}_z \rangle_s = \int_{S_E > 0} d\theta \int d\phi \sin \theta \cos \theta \left[ \int_{S_E > 0} d\theta \int d\phi \sin \theta \right]^{-1} \quad (4.7)$$

where

$$S_E = 2E + \omega_0 \cos \theta + \frac{g^2}{\Omega^2} \sin^2 \theta \cos^2 \phi \quad (4.8)$$

This last integration (4.7) must be performed numerically. We do this using a Monte Carlo integration method. The phase space average of  $\langle \hat{\sigma}_z \rangle$  is shown in Figs. 2–4 (solid line), together with the corresponding time average (dashed line) for different values of the energy and parameters of the system. The time average is done using the numerical solutions of the nonlinear equations of motion.

In Fig. 2 we depict a strong ( $g = 20$ ) resonant ( $\omega_0 = \Omega$ ) interaction for the spin-boson system. We can see that the average  $z$  component of the dipole is ergodic for a continuum of energy values, i.e., the time and phase space averages are essentially the same. Note that this is the chaotic regime for the semiclassical trajectories. This same behavior is evident in Fig. 3, where  $g = 11$ , but not in Fig. 4, where  $g = 5$ . In the latter case, when the largest Lyapunov exponent is very small, the deviation between time and phase space averages appears over most energy values. However, this deviation from ergodicity is not as marked as that in the nonresonant case shown in Fig. 5. In this latter figure there is no similarity between the two

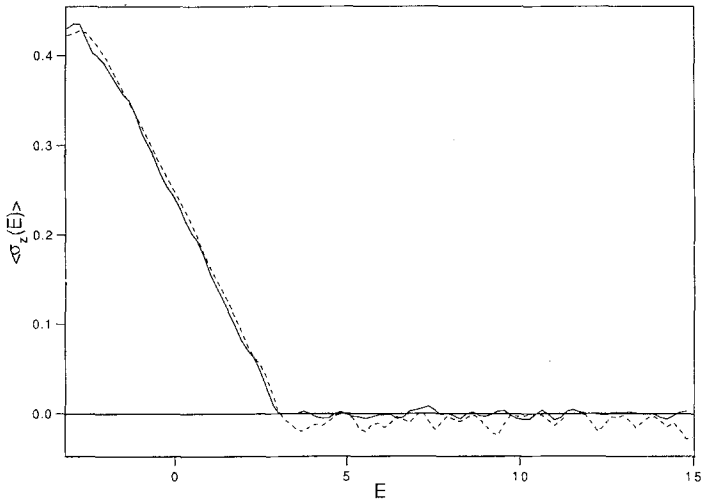


Fig. 2. Mean value of the  $z$  component of the dipole at the fixed energy  $E$  of the classical Hamiltonian corresponding to the set of equations (3.27). The full line is the theoretical prediction for the average over the microcanonical distribution. The dashed line is the numerical time average [see (4.3)]. The parameters used are  $g = 20$ ,  $\omega_0 = \Omega = 2\pi$ ,  $\bar{n} = 5$ .

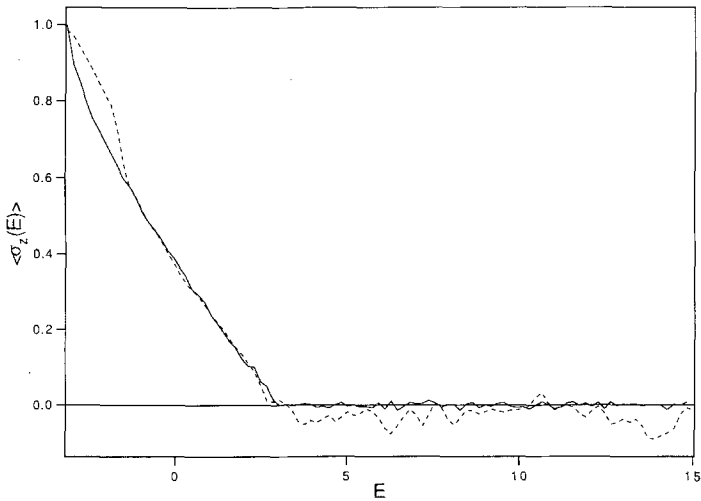


Fig. 3. Mean value of the  $z$  component of the dipole at the fixed energy  $E$  of the classical Hamiltonian corresponding to the set of equations (3.27). The full line is the theoretical prediction for the average over the microcanonical distribution. The dashed line is the numerical time average [see (4.3)]. The parameters used are  $g = 11$ ,  $\omega_0 = \Omega = 2\pi$ ,  $\bar{n} = 5$ .

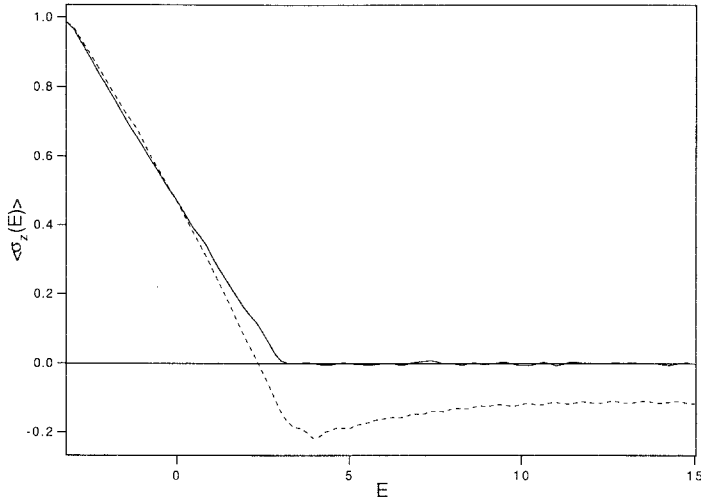


Fig. 4. Mean value of the  $z$  component of the dipole at the fixed energy  $E$  of the classical Hamiltonian corresponding to the set of equations (3.27). The full line is the theoretical prediction for the average over the microcanonical distribution. The dashed line is the numerical time average [see (4.3)]. The parameters used are  $g = 5$ ,  $\omega_0 = \Omega = 2\pi$ ,  $\bar{n} = 5$ .

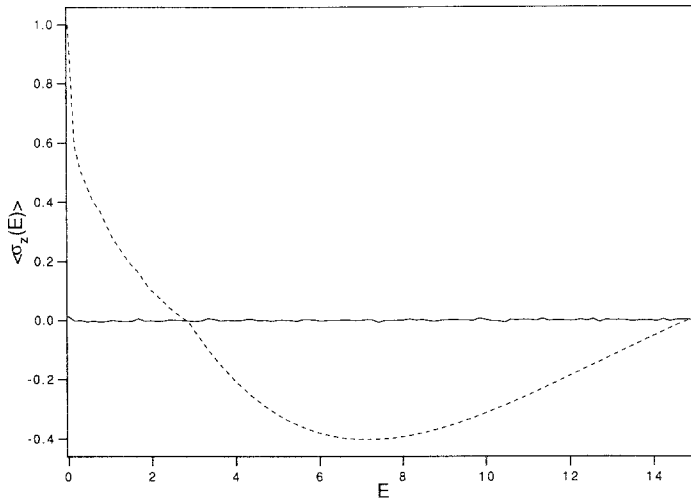


Fig. 5. Mean value of the  $z$  component of the dipole at the fixed energy  $E$  of the classical Hamiltonian corresponding to the set of equations (3.27). The full line is the theoretical prediction for the average over the microcanonical distribution. The dashed line is the numerical time average [see (4.3)]. The parameters used are  $g = 20$ ,  $\omega_0 = 0.01$ ,  $\Omega = 2\pi$ ,  $\bar{n} = 5$ .

averages. This means that the trajectories are constrained away from some regions of the energy surface in phase space. Note that this is the situation even in the case where the largest Lyapunov exponent is positive but small.

## 5. OTHER NUMERICAL RESULTS

Let us now turn our attention from the semiclassical equations (3.27) to the purely quantum system (3.24). We select an initial state in which the spin-1/2 dipole is in a pure state aligned along the  $z$  axis ( $x_3 = 1$ ) and the electric field is in a coherent state. The ensemble distribution for the initial state is then

$$\rho_w(\mathbf{x}, q, p; t=0) = \frac{1}{\pi} \exp\left\{-[\Omega^{1/2}q - (2\bar{n})^{1/2}]^2\right\} \\ \times \exp\left(-\frac{p^2}{\Omega}\right) \delta(x_3 - 1) \delta(x_2) \delta(x_1) \quad (5.1)$$

Note that the coherence assumption for the Bose field gives rise to a Gaussian distribution in both  $q$  and  $p$ , where  $\bar{n}$  is the average number of bosons in the field.

In Section 4, where we first discussed the numerical calculations, it became evident that the neglect of  $\mathcal{L}_{\text{QGD}}$ , the approximation made in going from the quantum phase space equations (3.24) to the semiclassical ones (3.27), is only valid for the system out of resonance and for small coupling strengths  $g$ . Of course this is precisely the parameter range where the semiclassical equations have regular trajectories for solutions.

In Fig. 5 we compare the average  $z$  component of the spin operator calculated using (3.24) and averaging over the initial distribution (5.1) with the theoretical prediction of Bonci, Grigolini, and Vitali (BGV).<sup>(19)</sup> The BGV prediction is closely related to the well-known treatment of quantum dissipation of Leggett and co-workers.<sup>(31)</sup> A detailed discussion of the merits and limitations of the former theoretical approach is given by Vitali and Grigolini,<sup>(32)</sup> who stress that in these latter approaches the reaction of the field to the evolution of the spin is neglected, thereby inadvertently suppressing important nonlinear effects. In Fig. 6a we observe that the interacting system without the backreaction yields a BGV prediction obtained from integrating the Liouville–von Neumann equations which coincides with averaging over the semiclassical trajectories using (3.22). Both calculations yield results for the spin-field system in which the boson field does not react and which is characterized by collapses and revivals. After an initial collapse followed by a long quiescent interval the average value of  $\hat{\sigma}_z$



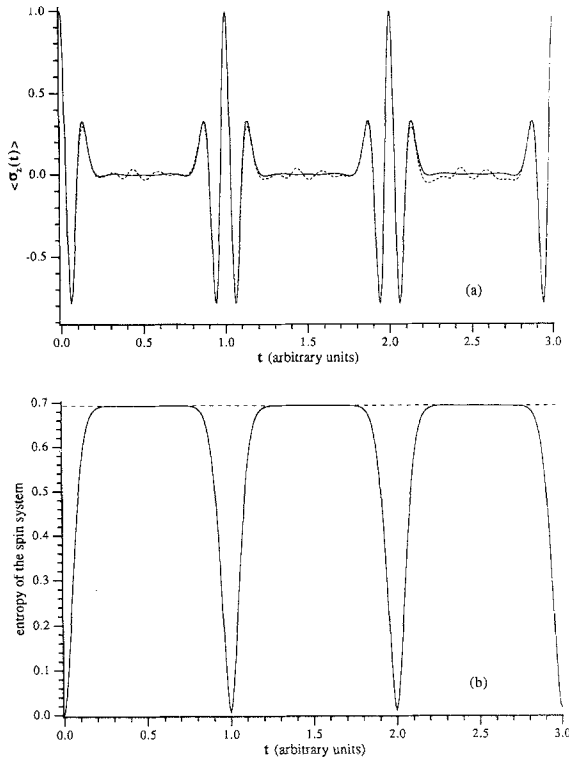


Fig. 6. (a) ... (b) Entropy of the spin-1/2 dipole as a function of time [see (5.3)]. The dashed line denotes the theoretical maximum value for the entropy. The parameters used are the same as those of (a).

suddenly begins to oscillate for a time and then collapses again. This behavior repeats again and again.

The phenomenon of collapse and revival is obtained via an averaging of different trajectories and is due to the quasiperiodic nature of the semiclassical trajectories leading to interference effects. Note that this classical system is not ergodic. According to the BGV interpretation, the collapse observed in Fig. 6a depends on a “multiplicative stochastic” process formally equivalent to Kubo’s stochastic coefficient (frequency) based on random fluctuations external to the system; in the present model the multiplicative fluctuations are generated by the dynamics of a single quantum oscillator. Semiclassical trajectories with different initial conditions are characterized by slightly different “oscillation frequencies” in the non-chaotic case and interference between these different members of the ensemble yields a Gaussian decay in time of the average spin-1/2 operators.

This functional form of the collapse was also obtained by Kubo<sup>(33)</sup> for his stochastic oscillator and by Cummings<sup>(34)</sup> for the JCM. It has therefore been concluded by a number of investigators that this phenomenon of collapse corresponds to a relaxation process. If it were a true relaxation process, however, the revival would not follow.

In any event our approximation scheme for the Wigner distribution does very well in following the results obtained from the numerical integration of the Liouville–von Neumann equation in the parameter regime far from resonance when the  $\hat{\mathcal{L}}_{\text{QGD}}$  term is neglected. It works well even for strong coupling ( $g=20$ ), which was not expected. However, this coincidence breaks down in the case of resonance.

In Fig. 7a the two procedures agree during the first collapse of  $\langle \hat{\sigma}_z \rangle$ ;

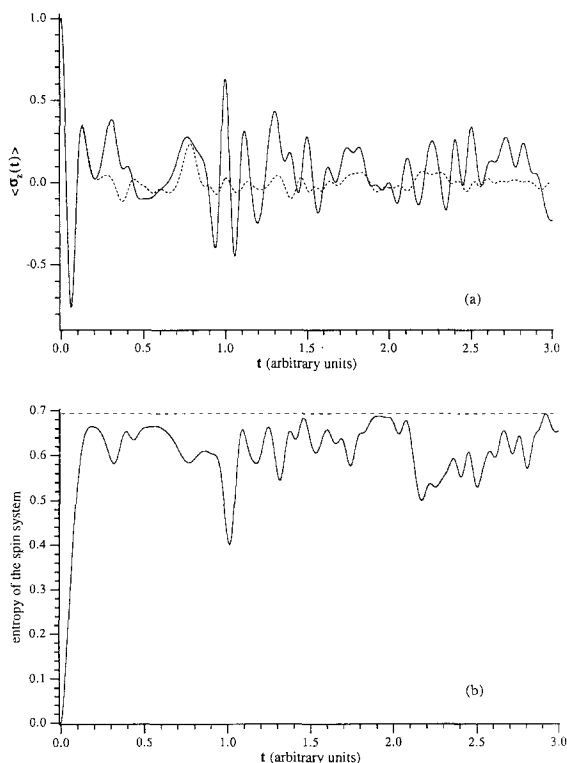


Fig. 7. (a) Mean value of the  $z$  component of the spin operator as a function of time. The solid curve is the prediction from the numerically integrated equation of motion; the dashed line is the result obtained by averaging the trajectories of (3.27) over the initial distribution of (5.1). The parameters used are  $g=20$ ,  $\omega_0 = \Omega = 2\pi$ ,  $\bar{n} = 5$ . (b) Entropy of the spin-1/2 dipole as a function of time [see (5.3)]. The dashed line denotes the theoretical maximum value for the entropy. The parameters used are the same as those of (a).

however, the subsequent predicted evolution of the system when  $\omega_0 = \Omega$  is quite different. It is apparent that in this parameter regime, where the semiclassical motion is chaotic, the averages over trajectories starting from different initial conditions give regular motion characterized by a relaxation process. Using the method of Benettin *et al.*, we evaluate the Lyapunov coefficient  $\lambda$ , which in the case of Fig. 7a turns out to be on the order of unity. It is worthwhile to point out that unlike the Kubo relaxation process discussed above, the decorrelation mechanism is here given by the internal dynamics of the spin-boson system rather than being external as in the stochastic fluctuations of Kubo.

As we said with regard to Fig. 7a, we depict two results of averaging in which the effects of chaotic trajectories are included. One uses (3.27), in which  $\mathcal{L}_{\text{QGD}}$  is neglected, and another takes the full Hamiltonian dynamics into account by numerical integration of the Liouville–von Neumann equations of motion. We refer to the latter as the exact calculation. We see in Fig. 7a that at the end of the standard relaxation process the system reaches a sort of thermodynamic equilibrium and that all revivals after the first are suppressed. It is clear that the collapse is now irreversible due to the subsequent incoherence of the chaotic trajectories. This is even more evident in the dashed curve for the average over the semiclassical trajectories, thereby not including the QGD.

The curve labeled exact in Fig. 7a includes the antidiffusional effects of QGD and shows a clear peak where the first revival is depicted in Fig. 6a. It has already been remarked that the QGD mechanism becomes essential in the presence of thermal fluctuations. It is possible to show that in the resonant case the QGD mechanism might be significant even in the case of weak spin–field coupling. Our numerical results indicate that the same parameter values that trigger chaos in the semiclassical trajectories also stimulate the QGD mechanism. We are thus lead to conclude that the QGD mechanism reacts against the spreading of chaotic trajectories, i.e., the relaxation process, and tends to recover, at least in part, the original correlations in the initial state.

We test the above interpretation by numerically integrating the Liouville–von Neumann equations for the density matrix and taking the trace over the field variables to obtain the spin density matrix  $\hat{\rho}_s(t)$ :

$$\hat{\rho}_s(t) = \text{Tr}_{\text{boson}} [\hat{\rho}(t)] \tag{5.2}$$

and defining the entropy for the spin-1/2 dipole as

$$S = - \text{Tr}_{\text{spin}} [\hat{\rho}_s(t) \ln \hat{\rho}_s(t)] \tag{5.3}$$

We see in Fig. 6b that the entropy  $S$  of the dipole subsystem monotonically increases until it reaches its maximum value ( $\ln 2 = 0.693$ ) at the end of the collapse process. However, once attained, the maximum entropy is eventually lost, the order of the spin system being restored by continued interaction with the boson field. The entropy monotonically decreases beyond its maximum to a minimum in the interval of the revival. This behavior of the entropy clearly indicates that the dynamics of the mixed state of the spin-1/2 dipole is reversible, i.e., it is not ergodic in this parameter regime.<sup>(15)</sup>

In Fig. 7b the entropy is calculated using the spin distribution, numerically determined by the full nonlinear dynamical equations, i.e., those in which the backreaction of the boson field is included. We note that the entropy monotonically approaches a plateau, as it should for an irreversible process. However, in the vicinity of the first revival, a ghost is observed in the form of a slight decrease in the entropy. This blip indicates a competition between the irreversible effects of chaos and the reversible effects of QGD, both of which are present in the *exact* calculation. It is clear, however, that in this case the effects of chaos are essentially irreversible.<sup>(15)</sup>

## 6. CONCLUSIONS

The generalized Wigner distribution is a useful tool for obtaining an approximation to the nonlinear dynamic equations describing the evolution of a quantum mechanical system. Using the spin-boson Hamiltonian, we found that in the far-from-resonance situation, this approximation recovers the *exact* quantum result. In the resonant case, that corresponding to the chaotic regime for the semiclassical trajectories, the Wigner method as used here breaks down. However, the technique provides a new insight into the evolution of quantum systems through the separation of the Liouville operator into the two parts  $\mathcal{L}_{cl}$  and  $\mathcal{L}_{QGD}$ .

In the above framework the semiclassical description of the system evolution is given by  $\mathcal{L}_{cl}$ . In certain parameter regimes we find that  $\mathcal{L}_{cl}$  leads to chaotic trajectories which in and of themselves lead to dissipation in the quantum domain due to interference in the appropriate averages. The second operator  $\mathcal{L}_{QGD}$  has a diffusionlike structure, but the state dependence of the “diffusion coefficient” results in its not being positive-definite and has been recently shown<sup>(14)</sup> to compete with thermal diffusion to fulfill the quantization prescription of quantum mechanics. This second operator provides the mechanism for the “quantum suppression of classical chaos” discussed in ref. 12. Let us contrast these results with the traditional

picture of a quantum system coupled to a heat bath. Quantum dissipation in these earlier models arises from the infinite number of degrees of freedom in the bath, which for technical reasons is generally treated as being linear (e.g., ref. 35). In the present paper, however, dissipation is found to also be a quantum manifestation of the chaos in the semiclassical trajectories. This latter dissipation has nothing to do with the traditional “heat bath” and is a consequence of the nonintegrability of the spin-boson Hamiltonian. Thus, quantum irreversibility is herein not a many-body effect, but rather one due to an implicit nonlinearity leading to chaos.

### APPENDIX

Herein we examine the degree of validity of the factorization approximation (3.25) by introducing the correlation function

$$C(t) = \langle \pi | [\exp(\hat{F}t)] \hat{q} | 3 \rangle - \langle \pi | [\exp(\hat{F}t)] \hat{q} | 0 \rangle \langle \pi | \exp(\hat{F}t) | 3 \rangle \quad (\text{A.1})$$

where the evolution operator is given by (3.18) and (3.14). The expansion of  $C(t)$  to increasing orders of the coupling parameter  $g$  is carried out as follows:

$$\begin{aligned} & \exp[(\hat{F}_0 + g\hat{F}_1)t] \\ &= [\exp(\hat{F}_0 t)] \left\{ 1 + \int_0^t [\exp(-\hat{F}_0 \tau)] g\hat{F}_1 \right. \\ & \quad \left. \times \exp[(\hat{F}_0 + g\hat{F}_1)\tau] d\tau \right\} \end{aligned} \quad (\text{A.2})$$

where the evolution operator has been separated into the two pieces

$$\begin{aligned} \hat{F}_0 &\equiv \left[ p \frac{\partial}{\partial q} - \Omega^2 q \frac{\partial}{\partial p} \right] - \omega_0 [ |2\rangle \langle 1| - |1\rangle \langle 2| ] \\ \hat{F}_1 &\equiv 2q [ p |3\rangle \langle 2| - |2\rangle \langle 3| ] - \frac{\partial}{\partial p} [ |0\rangle \langle 1| + |1\rangle \langle 0| ] \end{aligned} \quad (\text{A.3})$$

We introduce (A.2) into (A.1) and observe that the lowest order term in  $g$ , i.e.,  $g=0$ , has a vanishing correlation function:  $C(t; g=0)=0$ . The next-order terms in  $g$  are given by

$$\begin{aligned}
C(t) \cong & g \langle \pi | \int_0^t \{ \exp[-\hat{F}_0(\tau-t)] \} \hat{F}_1 \exp(\hat{F}_0 \tau) |3\rangle \\
& - g \langle \pi | \{ \exp[-\hat{F}_0 t] \} q |0\rangle \\
& \times \langle \pi | \int_0^t \{ \exp[-\hat{F}_0(\tau-t)] \} \hat{F}_1 \exp(\hat{F}_0 \tau) |3\rangle d\tau \\
& - g \langle \pi | \exp(\hat{F}_0 t) |3\rangle \\
& \times \langle \pi | \int_0^t \{ \exp[-\hat{F}_0(\tau-t)] \} \hat{F}_1 \exp(\hat{F}_0 \tau) |0\rangle d\tau + O(g^2) \quad (\text{A.4})
\end{aligned}$$

where, using (A.3), we obtain

$$\begin{aligned}
& [\exp(-\hat{F}_0 \tau)] F_1 \exp(\hat{F}_0 \tau) \\
& = 2g \left( q \cos \Omega t + \frac{p}{\Omega} \sin \Omega t \right) \\
& \quad \times [ (|3\rangle\langle 2| - |2\rangle\langle 3|) \cos \omega_0 t + (|3\rangle\langle 1| + |1\rangle\langle 3|) \sin \omega_0 t ] \\
& \quad - g \left( \frac{\partial}{\partial p} \cos \Omega t - \frac{\sin \Omega t}{\Omega} \frac{\partial}{\partial q} \right) \\
& \quad \times [ (|0\rangle\langle 1| + |1\rangle\langle 0|) \cos \omega_0 t + (|2\rangle\langle 0| - |0\rangle\langle 2|) \sin \omega_0 t ] \quad (\text{A.5})
\end{aligned}$$

Without writing out the explicit expressions for the correlation function to  $O(g^2)$ , it is clear that in the resonant case ( $\Omega = \omega_0$ ) the integrals over time in (A.4) result in secular terms. These terms remain bounded in the non-resonant case. In other words, when  $\omega_0 = \Omega$ , our factorization approximation neglects terms proportional to time and therefore is at best accurate for some small time interval. To be more precise, the method is correct when the coupling parameter is less than either of the two frequencies and the detuning parameter  $g < \Delta = |\omega_0 - \Omega|$ .

## ACKNOWLEDGMENT

We thank the Texas Higher Education Coordinating Board, Texas Advanced Research Program (TARP Project no. 003594-038), for partial support of this research.

## REFERENCES

1. T. Y. Li and J. A. Yorke, *Ann. Math. Mon.* **82**:985 (1975).
2. B. J. West, *An Essay on the Importance of Being Nonlinear* (Springer-Verlag, Berlin, 1985).

3. J. R. Buchler and H. Eichron, eds., *Chaotic Phenomena in Astrophysics*, *Ann. N.Y. Acad. Sci.* **497** (1987).
4. H. Bai-Lin, ed., *Directions in Chaos* (World Scientific, Singapore, 1987).
5. R. H. Enns, B. L. Jones, R. M. Muira, and S. S. Rangnekar, eds., *Nonlinear Phenomena in Physics and Biology* (Plenum Press, New York, 1981).
6. R. L. Devaney, *An Introduction to Chaotic Dynamical Systems*, 2nd ed. (Addison-Wesley, New York, 1989).
7. J. Guckenheimer and P. Holmes, *Nonlinear Oscillations, Dynamical Systems, and Bifurcations of Vector Fields* (Springer-Verlag, New York, 1983).
8. A. J. Lichtenberg and M. A. Leiberman, *Regular and Stochastic Motion* (Springer-Verlag, New York, 1983).
9. E. N. Lorenz, *J. Atmos. Sci.* **20**:130 (1963).
10. B. J. West, *Fractal Physiology and Chaos in Medicine* (World Scientific, Singapore, 1990).
11. R. M. May, *Nature* **261**:459 (1976).
12. T. Hogg and B. A. Huberman, *Phys. Rev. Lett.* **48**:711 (1982); S. Fishman, D. R. Gempel, and R. E. Prange, *Phys. Rev. Lett.* **49**:509 (1982); G. Casati, B. V. Chirikov, and D. L. Shepelyansky, *Phys. Rev. Lett.* **53**:2525 (1984); P. M. Koch, L. Moorman, B. E. Sauer, and E. J. Galvey, in *Classical Dynamics in Atomic and Molecular Processes* (World Scientific, Singapore, 1989).
13. M. Hillery, R. F. O'Connell, M. O. Scully, and E. P. Wigner, *Phys. Rep.* **106**:122 (1984).
14. R. Roncaglia, R. Mannella, D. Vitali, and P. Grigolini, unpublished.
15. L. Bonci, R. Roncaglia, B. J. West, and P. Grigolini, *Phys. Rev. Lett.* **67**:2593 (1991).
16. N. B. Nosozhmy, J. J. Sánchez-Mondragón, and J. H. Eberly, *Phys. Rev. A* **23**:236 (1981).
17. R. R. Puri and G. S. Agerwal, *Phys. Rev. A* **33**:3610 (1986).
18. S. M. Barnett and P. L. Knight, *Phys. Rev. A* **33**:2444 (1986).
19. L. Bonci, P. Grigolini, and D. Vitali, *Phys. Rev. A* **42**:4452 (1990).
20. J. Gea-Banacloche, *Phys. Rev. Lett.* **65**:3385 (1990).
21. H. Weyl, *Z. Phys.* **46**:1 (1927).
22. E. T. Jaynes and F. W. Cummings, *Proc. IEEE* **51**:89 (1963).
23. R. Graham and M. Höhnert, *Z. Phys.-Cond. Matter* **57**:233 (1984).
24. P. I. Belorov, G. M. Zaslavsky, and G. Th. Tartakovsky, *Sov. Phys. JETP* **44**:945 (1976).
25. P. M. Milonni, J. R. Ackerhalt, and H. W. Galbraith, *Phys. Rev. Lett.* **50**:966 (1983).
26. L. Allen and J. H. Eberly, *Optical Resonance and Two-Level Atoms*, Chapter 1 (Wiley-Interscience, New York, 1975).
27. A. Wolf, J. B. Swift, H. L. Swinney, and J. A. Vastarro, *Physica* **16D**:285 (1985).
28. G. Benettin, L. Galgani, and J. M. Strelcyn, *Phys. Rev. A* **14**:2338 (1976).
29. M. Berry, *J. Phys. A* **10**:2083 (1977).
30. A. Vorhos, in *Stochastic Behavior in Classical and Quantum Hamiltonian Systems*, G. Casti and J. Ford, eds. (Springer, New York, 1979).
31. A. J. Lettett, S. Chakravortz, A. T. Dorsey, M. P. A. Fisher, A. Gorg, and W. Zwerger, *Rev. Mod. Phys.* **59**:1 (1987).
32. D. Vitali and P. Grigolini, *Phys. Rev. A* **42**:4452 (1990).
33. R. Kubo, *J. Math. Phys.* **4**:174 (1963).
34. F. W. Cummings, *Phys. Rev. A* **140**:1051 (1965).
35. K. Lindenberg and B. J. West, *The Nonequilibrium Statistical Mechanics of Open and Closed Systems* (VCH Publishers, New York, 1990).